Rapid Back To Back Adenosine Stress/Rest Technetium-99m Teboroxime Myocardial Perfusion SPECT Using a Triple-Detector Camera

Terrance Chua, Hosen Kiat, Guido Germano, Kent Takemoto, Geraldine Fernandez, Yolanda Biasio, John Friedman and Daniel Berman

Departments of Imaging (Division of Nuclear Medicine) and Medicine (Division of Cardiology), Cedars-Sinai Medical Center; and the Department of Medicine and the Division of Nuclear Medicine and Biophysics, Department of Radiological Sciences, UCLA School of Medicine, Los Angeles, California

Technetium-99m-teboroxime is characterized by a high extraction fraction over a wide range of blood flow rates, rapid myocardial clearance and avid hepatic uptake. This study determined the imaging parameters and examined the clinical efficacy of a rapid back to back adenosine stress/rest teboroxime myocardial perfusion SPECT protocol using a triple-detector camera. Acquisition parameters were determined using cardiac phantom studies which were then applied in SPECT studies of 51 catheterized patients (22 with prior myocardial infarction) and 20 patients with a "low" (7.9% ± 4.3%) likelihood of coronary artery disease. Technetium-99m-teboroxime (20–25 mCi) was injected at the third minute of adenosine infusion. Teboroxime (20–25 mCi) was also injected at rest, 15 min later. Stress followed by rest SPECT were completed within 25 min using a triple-detector camera and sequential, 1-min continuous rotations in alternating directions. Summed raw data from the first to second (1–2 min), second to third (2–3 min) and second to fifth (2–5 min) minutes of imaging following stress teboroxime injection were reconstructed and compared for image quality, degree of liver interference, and accuracy for diagnostic efficacy. In a subgroup of 30 patients, 2-8-min summed images were also reconstructed to compare this more conventional imaging protocol with our rapid acquisition. Image quality was fair to good in 75% of the 1–2-min, 84% of the 2–3-min and 2–5-min studies and 53% of the 2–8-min scans. The frequency of severe liver interference appeared to increase with the duration of imaging time (1–2 min: 3%; 2–3 min: 7%; 2–5 min: 8%) and was greatest (30%, p = 0.08) with 2–8-min images. Three patients (4%) had uninterpretable studies due to intense hepatic uptake. Overall sensitivity (95%) and specificity (71%) were equal for the 2–3-min and 2–5-min stress images and appeared better than in the 1–2-min images (84% and 57%, respectively). For the 2–8-min scans, vessel sensitivity (69%) and specificity (63%) appeared poorer than with 2–3-min studies (83% and 81%, respectively). Normalcy rates were 89% for the 2–3-min and 2–5-min and 79% for 1–2-min images. The back to back adenosine stress/rest teboroxime SPECT can be performed in 30 min using a triple-detector camera. Although overall high sensitivity and normalcy rates were achieved, the protocol is technically demanding. Interference due to intense liver uptake remains problematic.

J Nucl Med 1993; 34:1485–1493

Teboroxime (Cardiotec, SQ30217) is a technetium-based myocardial perfusion imaging compound classified as a boronic acid adduct of technetium oxime (BATO) (*1*). Among its unique features are a high extraction fraction (>90%) even at high coronary flow rates and rapid myocardial washout (*2–4*) which allows for short intervals between stress and rest injections. The rapid myocardial washout of teboroxime coupled with its intense late hepatic uptake necessitates that imaging be completed more quickly than with ^{201}Tl or ^{99m}Tc sestamibi. Accordingly, we hypothesized that optimal tomographic imaging with teboroxime could be accomplished using a multi-detector camera to maximize counting statistics. In addition, adenosine pharmacologic stress performed with the patient already positioned under the camera eliminates delays between tracer injection and the start of acquisition, resulting in better image statistics.

The purpose of this study was twofold; first, to determine the optimal imaging parameters for rapid back to back adenosine stress/rest teboroxime single-photon-emission computed tomography (SPECT) using a triple-detector camera; and second, to assess the overall accuracy of this approach for detection of coronary artery disease.

Received Dec. 14, 1992; revision accepted May 11, 1993.

For correspondence or reprints contact: Daniel S. Berman, MD, Co-Director, Dept. of Imaging, Cedars-Sinai Medical Center, 8700 Beverly Blvd., Los Angeles, CA 90048.

TABLE 1
Study Population Demographics

	CATH	LL
Number of patients	51	20
Male/female ratio	23/28	8/12
Mean age (yr)	73.7	62.8
Prior infarct	22	—
Single-vessel disease	16	—
Double-vessel disease	14	—
Left main/triple vessel	13	—
Uninterpretable*	2	1

*All due to intense liver uptake.
CATH = catheterized patients; LL = low likelihood patients.

METHODS

Study Population

The study population consisted of 71 patients referred to our laboratory for myocardial perfusion imaging using pharmacologic stress between January 1991 and December 1991. Of this population, 51 patients underwent coronary angiography within 3 mo of adenosine teboroxime SPECT and 20 were considered to have a low likelihood of coronary artery disease. Patients with asthma, second or third degree heart block, hypotension, cardiomyopathy or prior coronary bypass surgery were excluded. Table 1 summarizes the clinical features of the study patients. The pretest likelihood of disease in the low likelihood patients was 7.9% ± 4.3% (range 0.8% to 16.1%), based on age, gender, risk factors and symptom classification as calculated by the system of Diamond and Forrester using the computer program CADENZA (*5–7*). Twenty-two of the catheterized patients had a prior history of myocardial infarction.

Six patients had undergone prior angioplasty and in two, angiography was repeated in proximity to the nuclear study (7 days and 31 days before SPECT). These two patients were included in the analysis of sensitivity and specificity. The other four angioplasty patients were included only for analysis of image quality and liver interference. All patients were required to abstain from xanthine derivatives for at least 48 hr and caffeine for 24 hr prior to the study and signed a consent form approved by the Institutional Review Board of the medical center.

Cardiac Phantom Study Protocol

To identify the optimal imaging parameters to be used with Tc-teboroxime, cardiac phantom studies were performed using a modified commercial chest phantom (Data Spectrum 2230 with cardiac insert 7070) with a wedge-shaped lucite insert to simulate the liver. Technetium-99m was introduced into the cardiac insert (4.4 μCi/ml), the liver insert (3.4 μCi/ml) and background (0.9 μCi/ml) to simulate the counts distribution in a typical teboroxime study. A defect (4-cm^3 fillable chamber) was positioned in the lateral wall of the cardiac insert. With the phantom's location accurately kept constant by means of a laser alignment system, sequential acquisitions were performed while varying the following parameters: collimator (low-energy, high-resolution versus low-energy, general all-purpose), zoom (1, 1.33, 1.6), orbit (circular versus noncircular) and method of acquisition (continuous versus step and shoot). Images were reconstructed with a low-pass Butterworth filter, order 5.0, using various cut-off frequencies (0.15, 0.20, 0.25, 0.3 of Nyquist).

All resliced short-axis images were compared visually and with a performance index calculated as the product of myocardial uniformity and defect contrast.

To calculate defect contrast, three regions of interest (ROIs) were drawn using the interactive software package Explorer (*8*). The first two (ROI_{heart} and ROI_{lesion}), which were circular in shape, were centered on the anterior myocardial wall and on the defect, respectively. The third ROI (ROI_{bkg}), in the shape of a crescent moon, was positioned adjacent to the anterior myocardial wall. The three ROIs were automatically applied to all short axis images analyzed and the average counts/pixel calculated for each ROI. Then, the heart-to-lesion and heart-to-background contrast was calculated, and the defect contrast obtained as their product.

$$CONTRAST_{heart\text{-}lesion} = \frac{(ROI_{heart})_{ave} - (ROI_{lesion})_{ave}}{(ROI_{heart})_{ave}} \quad \text{Eq. 1}$$

$$CONTRAST_{heart\text{-}bkg} = \frac{(ROI_{heart})_{ave} - (ROI_{bkg})_{ave}}{(ROI_{heart})_{ave}} \quad \text{Eq. 2}$$

$$CONTRAST = CONTRAST_{heart\text{-}lesion} \cdot CONTRAST_{heart\text{-}bkg}. \quad \text{Eq. 3}$$

Myocardial count uniformity was assumed to be inversely proportional to the average fractional root-mean-square (rms) noise in 12 ROIs distributed over 270° of normal myocardium. The rms noise was calculated for each ROI as the ratio of the standard deviation (s.d.) to the average counts in the ROI.

$$\text{rms noise} = \sum_i \frac{SD_i}{(ROI_i)_{ave}} \quad \text{Eq. 4}$$

$$\text{Uniformity} = \frac{1}{1 + \left(\frac{\text{rms noise}}{0.14}\right)^{14}} \quad \text{Eq. 5}$$

$$\text{Performance Index} = CONTRAST \cdot \text{Uniformity}. \quad \text{Eq. 6}$$

Equation 5 is a Butterworth recursive filter function which asymptotically approaches y = 1 for low noise, y = 0 for high noise and is smooth elsewhere. It reflects the fact that the perceived uniformity of myocardial uptake is excellent for rms percent noise levels of up to 10%, then rapidly deteriorates. As stated above, the performance index was calculated as the product of myocardial uniformity and defect contrast.

All of the phantom experiments were performed with the same triple-detector camera (Prism 3000, Picker International, Cleveland, OH) used for the clinical study.

Clinical Study Protocol

The clinical protocol is summarized in Figure 1. Two separate intravenous lines were inserted. The patient was positioned under the triple-detector gamma camera before commencement of pharmacologic stress. Adenosine (Adenoscan, Medco, Los Angeles, CA) was infused at 140 μg/kg/min and continued for 6 min in 20 patients and 4 min in the remaining 31 patients. Teboroxime (20–25 mCi) was injected at the third minute of adenosine infusion. The abbreviated 4-min adenosine protocol was instituted based on the rationale that (1) peak coronary blood flow with intravenous adenosine is reached by 3 min; (2) teboroxime blood clearance is rapid; and (3) accelerated myocardial tracer washout during prolonged maximal hyperemia might result in reduced

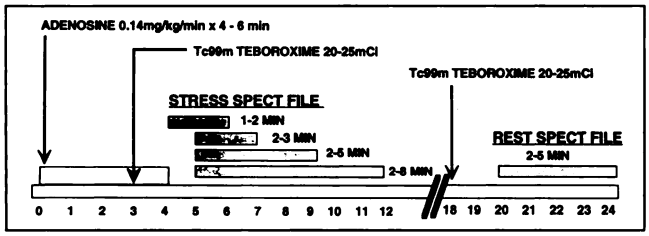

FIGURE 1. Clinical protocol for back to back adenosine stress/rest teboroxime SPECT.

myocardial counts, thereby degrading image quality. Between 15 and 20 min after stress injection, 20–25 mCi of teboroxime was injected (rest injection). Sequential 1-min SPECT files were acquired using a low-energy, high-resolution collimator with the detector rotating with continuous motion in alternating directions, beginning 1 min after stress teboroxime injection and ending 5 min after rest teboroxime injection. Data collection proceeded in 3° steps over 360°.

Image Processing

Stress tomographic images were reconstructed using summed raw data (planar) images from the first to second minute (1–2 min), second to third minute (2–3 min) and second to fifth minute (2–5 min) post-teboroxime injection. In a subgroup of 30 patients, we also summed second to eighth minute (2–8 min) stress planar data to compare more conventional imaging protocols against rapid (2–3 min) acquisition. Four-minute rest planar images were built by summing planar data from the second to the fifth minute after rest injection. Based on the phantom study and our initial experience in patient studies, summed planar data from clinical studies were pre-filtered with a low-pass filter (Butterworth, order 5, cutoff 0.215 Nyquist) and reconstructed via filtered backprojection with a ramp filter. Transaxial tomograms were reoriented into horizontal long-axis, vertical long-axis and short-axis views. All image reconstruction used the 180° data from the 45° left posterior oblique to the 45° right anterior oblique projections without attenuation correction.

Image Interpretation for Clinical Studies

Reconstructed short-axis stress images (1–2 min, 2–3 min, 2–5 min, 2–8 min) and the 2–5-min rest images were interpreted separately by two observers blinded to the results of coronary angiography using a five-point scoring system (0–4 = normal to absent tracer uptake) for 20 tomographic segments of the left ventricular myocardium, as previously described (*9,10*). Image quality was subjectively assessed using a four-point system (1–4: poor, fair, good, excellent), based on visual myocardial-to-background activity ratios, left ventricular endocardial and epicardial border definition and contrast of perfusion defects. In addition, the degree of liver interference was assessed (1–4: severe, moderate, mild, absent) based on hepatic uptake intensity and liver proximity to the left ventricular wall.

Coronary Angiography

Cardiac catheterization was performed by the standard Judkins technique. Coronary angiograms were visually interpreted by two experienced observers blinded to the results of the teboroxime study. Significant coronary artery disease was defined as ≥50% stenosis in a major epicardial artery.

Statistical Analysis

The normalcy rate was defined as the number of patients in the low likelihood group with normal scintigraphic patterns divided by the total number of patients in the low likelihood group. The term normalcy rate is used to distinguish this group from the group conventionally used for specificity based on normal coronary arteriograms (*5–7*). Comparisons of proportions were made with the use of chi-square statistics or, when appropriate, Fisher's exact test. The mean differences for continuous variables were compared using the Student t-test. All continuous measures were summarized as the mean value ± s.d. The alpha level of significance was set at 0.05. All computations were made with the True Epistat statistical software (*11*).

RESULTS

Cardiac Phantom Studies

When the quantitative values of the performance index were compared for the low-energy, high-resolution (LEHR) and general, all-purpose (GAP) collimator, the former proved superior at all zooms and cutoff frequencies tested. Total myocardial counts were 25% greater and the count uniformity somewhat better with the GAP, but defect contrast was 10%–20% lower than with the LEHR. For either collimator at any cut-off frequency, defect contrast was 10%–50% lower with a zoom of 1, compared to a zoom of 1.33 or 1.6. For all combinations of zoom, collimators and cut-off frequencies, there was no significant difference in contrast or uniformity using continuous versus step and shoot acquisition. However, 1 min of actual data collection in 3° steps over 360° (40 steps/detector) required 2.3 min in step and shoot versus 1 min in continuous acquisition mode. No significant differences in the performance index were measured for noncircular versus circular acquisition orbits, although the former resulted in somewhat better lesion contrast and lower uniformity. All the quantitative findings were confirmed by visual analysis.

The highest values for the performance index were obtained with LEHR collimation, zoom of 1.33 or 1.6 and pre-filter cutoff of 0.20–0.25 cycles/pixel. The 1.6 zoom yielded the best image quality overall in that frequency cut-off range, although our initial clinical experience in the back to back stress/rest teboroxime protocol (*12*) suggests that the 1.33 zoom should be chosen to ensure that the camera's field of view is large enough to completely encompass the patient's heart throughout the acquisition.

Patient Studies

Image Quality. The relationship between reconstructed image quality and imaging time (1–2 min, 2–3 min, 2–5 min, 2–8 min) is shown in Figure 2. The quality of the 2–5-min images was judged to be excellent in 6/71 (8%), good in 32/71 (45%), fair in 28/71 (39%) and poor in 5/71 (7%) of the studies. The 1–2-min time frame appeared to contain a higher proportion of lower quality images associated with evidence of residual blood pool activity on the projection data. However, these differences were not statistically significant. For the rest teboroxime studies, the quality of the 2–5-min images was considered excellent, good, fair and poor in 7%, 55%, 33% and 5% of the studies, respectively (p = NS for each category compared to the 2–5-min stress images).

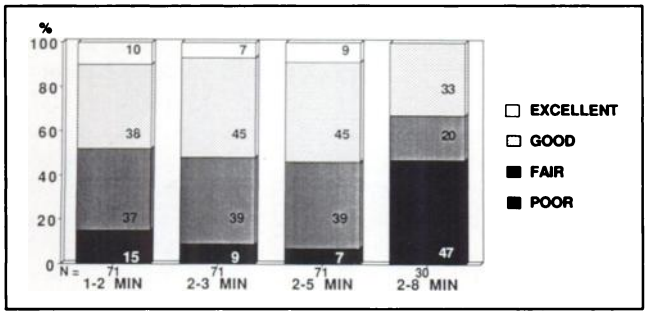

FIGURE 2. Relationship between image quality and imaging duration in clinical studies. The figures reported in the bar graphs indicate the percentage of studies associated with the respective image quality (from excellent to poor). The figures below each bar indicate the number of patient studies for each imaging duration.

In the subgroup of 30 patients in which 2–8-min stress images were evaluated, 53% (16/30) of the 2–8-min images were of fair to good quality, compared to 87% (26/30) of the 2–3-min images in the same 30 patients ($p < 0.01$). Poor image quality occurred in 47% (14/30) of the 2–8-min images, as compared to 10% (3/30) of the 2–3-min images ($p < 0.004$). Four (13%) of the 2–8-min images were uninterpretable, compared to one (3%) of 2–3-min images (p = NS).

When 6-min and 4-min adenosine infusions were compared, the proportion of poor studies appeared to be higher with the 6-min infusion (3/20 or 15% of studies versus 3/51 or 6%), although these differences did not reach statistical significance.

Liver Interference. The relationship between the degree of liver interference and imaging time is shown in Figure 3. Liver interference was judged to be severe in 3%–8% of studies. The 1–2-min studies appeared to have a lesser degree of liver interference compared to the 2–3-min and 2–5-min studies although these differences were not statistically significant. Three of seventy-one patients (4%) had uninterpretable studies due to severe liver interference (one patient had a low pretest likelihood of coronary artery disease; another had previous myocardial infarction and the other had coronary artery disease but no previous infarction). For the rest teboroxime studies, the degree of liver interference of the 2–5-min images was considered

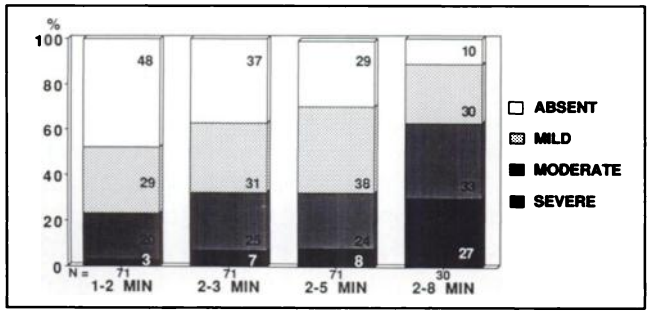

FIGURE 3. Relationship between the degree of liver interference and the imaging duration in clinical studies. The figures reported in the bar graphs indicate the percentage of studies associated with that degree of liver interference. The figures below each bar indicate the number of patient studies for each imaging duration.

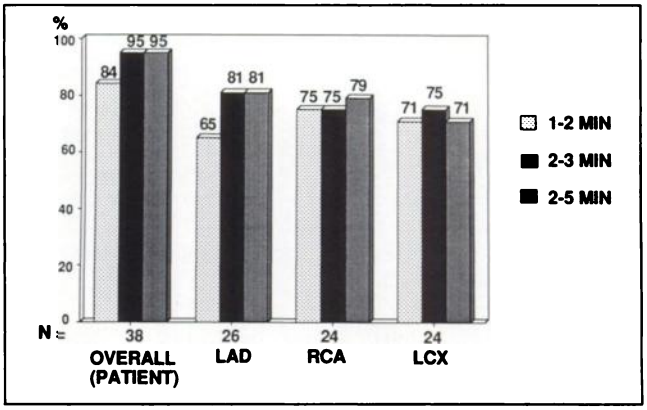

FIGURE 4. Comparison of the sensitivities for detection of coronary artery disease, obtained using the three different imaging durations. LAD = left anterior descending, RCA = right coronary artery, LCX = left coronary artery.

severe, moderate, mild and absent in 5%, 27%, 40% and 28% of the studies, respectively (p = NS for each category compared to the 2–5-min stress images).

In the subgroup of 30 patients in which 2–8-min stress images were evaluated, severe liver interference occurred in 27% of the 2–8-min images, compared to 7% (2/30) of both the 2–3-min and 2–5-min images ($p = 0.086$) and 3% (1/30) of 1–2-min studies ($p = 0.025$).

Finally, there was a trend towards greater liver interference in the studies with 6-min adenosine infusions, compared to the 4-min adenosine infusions, which did not achieve statistical significance (10% versus 6%).

Sensitivity, Specificity and Normalcy Rates. Figure 4 compares the sensitivity for detection of coronary artery disease as derived for the 1–2-min, 2–3-min and 2–5-min summed, short-axis stress images. In the 2–3-min and 2–5-min images, overall (patient) sensitivity for detecting disease was 95%. In the same images, vessel sensitivities were 81% for the left anterior descending artery, 75%–79% for the right coronary artery and 71%–75% for the left circumflex artery. When the patients with previous myocardial infarction were excluded, the overall sensitivity was 16/18 (89%). The overall and vessel sensitivities for the detection of coronary artery disease tended to be slightly lower in the 1–2-min images.

Figure 5 compares the normalcy rate and specificity of the 1–2-min, 2–3-min and 2–5-min summed images. In the 2–3-min and 2–5-min images, the overall specificity was 71% (5/7), the normalcy rate 89% and the vessel specificity 84% for the left anterior descending, 81%–86% for the right coronary artery and 95% for the left circumflex artery. The overall specificity, normalcy rate and vessel specificities for the detection of disease tended to be lower in the 1–2-min images.

When the overall sensitivity and specificity were analyzed based on the duration of adenosine infusion, there was no significant difference in either sensitivity (76% for 4 min versus 80% for 6 min) or specificity (87% for 4 min

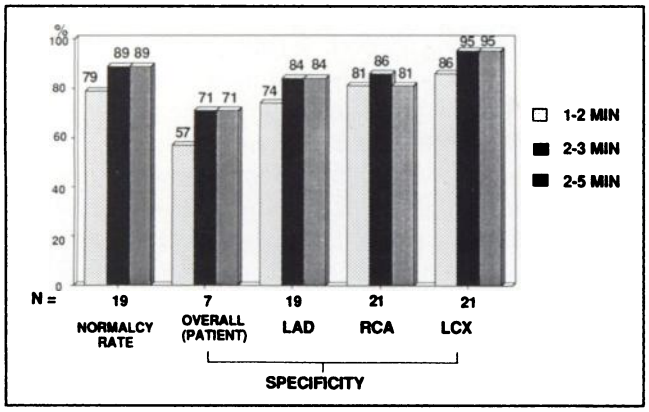

FIGURE 5. Comparison of the normalcy rate and specificity for detection of coronary artery disease, obtained using the three different imaging durations. LAD = left anterior descending, RCA = right coronary artery, LCX = left circumflex artery.

versus 91% for 6 min) for the detection of individual vessel disease.

The above analyses of sensitivity, specificity and normalcy rates are based on the patients with interpretable studies or 96% of the total. Two of the three patients with uninterpretable studies had significant coronary artery disease. If these patients were included in the analyses and considered as having negative scan results, the sensitivity would remain high at 92% for the entire patient population and 84% for the subgroup of patients with no previous infarction.

In the subgroup of patients in which the 2–8-min images were examined, those images were uninterpretable in four patients (15%). In the remaining patients, overall patient sensitivity was 75% for the 2–8-min images versus 90% for the 2–3-min images (p = ns). Vessel sensitivity (69%) and specificity (63%) also appeared poorer with the 2–8-min compared to the 2–3-min images (83% and 81%, respectively, p = ns).

Case Examples

Figure 6 is an example of a normal adenosine stress/rest teboroxime study reconstructed from 2-min to 5-min summed stress and rest projection data. Note the uniform distribution of the tracer throughout the myocardium.

Figure 7 illustrates the difference between the 1–2-min, 2–3-min, 2–5-min and 2–8-min stress images from a patient with left anterior descending and left circumflex disease.

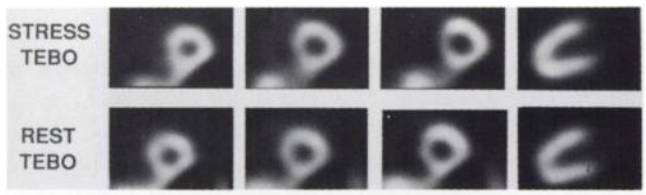

FIGURE 6. Case Example: Normal. Representative apical, mid-ventricular and basal short axis (left) and mid-vertical long axis (right) stress and rest images of a patient with a low likelihood of coronary artery disease. Note the uniform distribution of tracer throughout the myocardium. This image was reconstructed from the sum of 4 min of projection data.

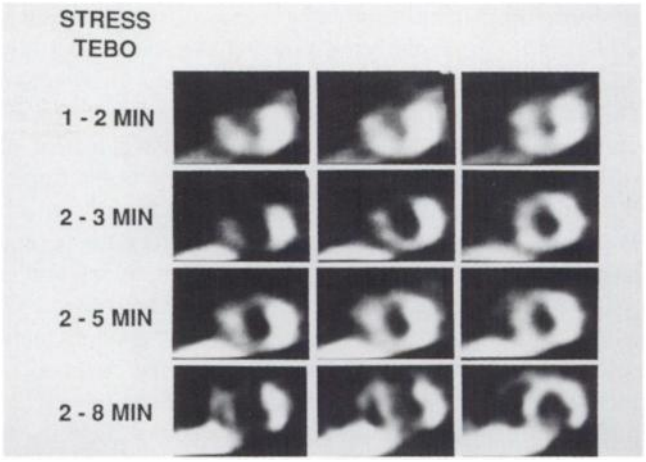

FIGURE 7. Case Example: Different Imaging Times. 1–2 min, 2–3 min, 2–5 min and 2–8 min summed short axis stress images (top to bottom) of a patient with left anterior descending and left circumflex disease. The image display format is identical to Figure 6. Liver activity increases as the acquisition progresses, becoming very intense in the 2–8-min images. In contrast, the 1–2-min images have little hepatic activity, but image quality is poorer because of residual blood pool activity.

Note the presence of perfusion defects in the anterior, anteroseptal and inferior wall, visible on all images. Liver activity increases with the duration of imaging time, becoming very intense in the 2–8-min images. Although liver activity is minimal in the 1–2-min images, the definition of the myocardial cavity and borders is poorer than in the 2–3-min and 2–5-min images, due to residual blood-pool activity.

Figure 8 is an example of an adenosine stress/rest study rendered uninterpretable by intense liver uptake. There are stress perfusion defects in the anterior and inferior wall. Since intense liver activity adjacent to the heart can give rise to a paradoxical decrease of counts in the inferior wall in the absence of a perfusion abnormality (*13*), interpretation of the inferior wall findings in this patient could not be made with confidence. This patient was found to have triple-vessel disease on angiography.

DISCUSSION

Our study has served to develop, optimize and validate a rapid, back to back stress/rest ^{99m}Tc-teboroxime SPECT

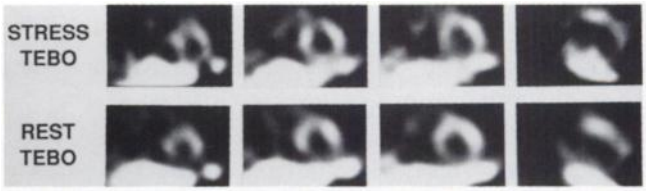

FIGURE 8. Case Example: Liver Interference. This study of a patient with triple vessel disease was rendered uninterpretable by severe liver interference. The image display format is identical to Figure 6. There are defects in the anterior and inferior wall on the 2–3-min short axis image, but the diagnosis could not be made with confidence because intense liver uptake is sometimes associated with an artifactual decrease in inferior wall counts.

protocol in combination with adenosine pharmacologic stress and a triple-detector camera. We chose to study teboroxime because of its very high myocardial extraction at high flow rates and its rapid washout from the myocardium. The former offers great potential for detection of early or mild disease, while the latter permits the implementation of a rapid back to back stress and rest protocol. We chose a triple-detector camera because it was the only camera in our laboratory capable of continuous rotation at that time, an acquisition mode most suitable for dynamic SPECT studies. Pharmacologic stress was used to minimize delays between tracer injection and the commencement of image acquisition since the patient can be readied under the camera prior to stress testing. Additionally, if exercise stress had been used, the implementation of a rapid protocol would have conflicted with the necessity to avoid inferior wall artifacts caused by the upward creep of the heart (*14*). Adenosine was employed because of its demonstrated maximal hyperemic effect and brief duration of action (*15*).

Acquisition and Reconstruction Parameters

The appropriate acquisition and reconstruction parameters (LEHR collimator, continuous acquisition along a noncircular orbit, zoom of 1.33, pre-filtering with a Butterworth filter of order 5 and cutoff of 0.215 cycles/pixel, reconstruction with a ramp filter) were selected based on the results of the cardiac phantom experiments and our clinical study experience.

The poorer lesion contrast with a zoom of 1 compared to 1.33 or 1.6, is linked to sampling considerations, since the image matrix size (64 × 64 pixel^2) does not change. With a zoom of 1.33 or 1.6, a smaller area of the camera's field of view is mapped to the 64 × 64 matrix, thus the pixel size is smaller and the spatial resolution better than with a zoom of 1. For the defect simulated in the phantom experiment, both zoom 1.33 and zoom 1.6 provide adequate sampling.

Continuous acquisition was chosen to avoid the dead time associated with the stepping process in the step and shoot mode where acquisition is suspended every time the detector(s) steps from one projection to the next. Continuous acquisition is probably of greater importance to our protocol than the use of the triple-detector camera. Using a single-detector camera with continuous acquisition, Burns et al. (*16*) have shown that 3-min teboroxime SPECT studies provide comparable sensitivity and specificity to a 20-min ^{201}Tl study. For the same count statistics, use of triple-detector cameras further reduces imaging time (by a factor of one-third for 180° reconstruction).

Optimal Imaging Time

The use of a triple-detector camera and continuous rotation allowed us to perform dynamic SPECT acquisitions as sequential 1-min rotations in alternating directions. Planar data from various numbers of adjacent 1-min temporal frames could be summed together before reconstruction, thus permitting an evaluation of the effect of imaging time on image quality and detection of disease. Our results showed that the optimal imaging period was between 2 min and 5 min following injection of teboroxime. The presence of residual blood pool activity in images acquired earlier than 2 min generally resulted in poorer image quality and lower overall sensitivity and specificity in the 1–2-min images. On the other hand, later images show a greater degree of hepatic activity, since the tracer accumulates in the liver at a relatively slow rate. Analysis of the subgroup of 30 patients with 2–8-min images demonstrated severe liver interference in 27% (8/30) of the studies and significantly poorer image quality compared to the shorter imaging intervals.

Prolonged imaging also presents the potential risk of loss of defect contrast and lower disease detection rate due to differential tracer washout. Animal (*17*) and clinical (*18*) studies have demonstrated that teboroxime clearance is related to blood flow. Tracer washout is slower in the ischemic myocardium compared to the normal myocardium, causing a reduction in defect contrast over time. A varying tracer concentration during acquisition has also been shown to cause image artifacts in phantom experiments and computer simulations. Bok et al. (*19*) have suggested that image distortion is not significant if the total imaging time is less than the effective half-life of the tracer in a 360° SPECT acquisition. However, their work was qualitative rather than quantitative and assumed a uniform rate of washout of teboroxime between normal and ischemic myocardium, which in fact is not the case (*17,18*). Links et al. (*20*) performed a computer simulation employing washout values obtained from canine studies and showed that image artifacts were produced when the SPECT acquisition was longer than 3 min. Similarly, O'Connor et al. (*21*) studied the effects of a range of washout rates on circumferential myocardial profiles and found that, based on known washout rates, teboroxime SPECT studies need to be completed within 2–4 min. These conclusions were based on acquisition with a single-detector SPECT camera performing a single rotation. Multiple continuous camera rotations in alternating directions, as in our protocol, may reduce image artifacts because each individual rotation is accomplished in just 1 min and even if data from successive 1-min frames are summed, the effect of the direction of rotation would tend to be canceled out. The concept of decreased artifacts with an alternating direction of rotation is supported by the work of Nakajima et al. (*22*).

It is of interest to note that, with respect to image count statistics obtained with the triple-headed camera, the 2–3-min and 2–5-min anterior view adenosine teboroxime (20–25 mCi) images contain 8,000–9,000 and 12,000–15,000 myocardial counts, respectively. Using the same triple-head camera and the routine clinical acquisition time of 15 min for ^{201}Tl (3 mCi) and ^{99m}Tc sestamibi (20 mCi) yield 20,000–25,000 and 45,000–50,000 myocardial counts, respectively. Thus, despite the use of a triple-head detector camera and continuous acquisition, teboroxime studies with this fast protocol result in relatively low-count images.

Duration of Adenosine Infusion

Although evaluating the duration of adenosine infusion was not the main purpose of this study, we found the 4-min infusion to be preferable to the 6-min infusion (injection of teboroxime was performed at the third minute in both cases). Adenosine hyperemia has been shown to be maximal within 2 min of starting infusion and is abolished 2.5 min after the infusion is stopped (*15*). Moreover, extraction of teboroxime is high at the first pass, but may be reduced at subsequent passes by its binding characteristics to blood cells and plasma proteins (*23*). Thus, there seems to be little reason to prolong the length of adenosine infusion; in fact, a longer infusion time increases the duration of the patient's symptoms and heightens the risk of patient motion. Finally, prolonging the duration of adenosine-induced hyperemia would increase the rate of tracer washout from the myocardium and lower count statistics, while increasing the effect of differential washout and reducing defect contrast. Poor image quality was slightly but not significantly more frequent with the 6-min (3/20 or 15%) than with the 4-min infusion (3/51 or 6%), while sensitivity and specificity were similar for the two protocols.

Sensitivity and Specificity

The sensitivity for detection of coronary artery disease was high (95%) in the study population (three patients with uninterpretable studies were excluded). In patients without prior infarction, sensitivity was 90%. With regard to specificity, there were only a small number (n = 7) of patients with normal coronary arteries on angiography, as might be expected in a clinical situation where the patients referred for cardiac catheterization are those with abnormal test results. Five out of seven patients with normal coronaries had normal studies (specificity = 71%), confirming results previously reported for teboroxime SPECT. Fleming et al. (*24*) reported sensitivity of 94% (16/17) and specificity of 75% (6/8) for exercise stress teboroxime SPECT studies using a single-detector camera with step-and-shoot acquisition. Iskandrian et al. (*25*), using a single-detector camera and adenosine-induced stress, also reported that 15 of 16 (94%) patients with coronary artery disease had abnormal teboroxime SPECT studies and two of four normal patients had normal teboroxime studies.

Patients with normal perfusion studies are usually not referred for catheterization and this post-test referral bias tends to lower specificity for detection of coronary artery disease (*26*). To overcome the limitation presented by the small number of patients with normal angiograms, we have used the normalcy rate (*27*) as a proxy of specificity. The normalcy rate is defined as the frequency of normal test results in patients clinically referred for stress testing and with a low (<5%) pretest likelihood of coronary artery disease. In this study, the normalcy rate was high (89%), but not different from recently reported figures for normalcy rates in stress-redistribution SPECT thallium (*28*). Of note, the likelihood of coronary artery disease in the low likelihood population of this study is higher than that of our previous work with stress studies, since most of the patients in the present study could not undergo exercise ECG testing.

Since intense liver activity adjacent to the heart can lead to paradoxical decrease of counts in the inferior wall in the absence of perfusion abnormalities (*13*), test specificity could be affected by a false-positive inferior wall defect on stress (and rest) images. In this study, we observed that when significant liver interference was present, it affected both the stress and rest images to a similar degree by visual interpretation. Therefore, the likely false-positive finding as a result of liver interference is that of a nonreversible inferior wall defect. The impact of various degrees of liver interference in the production of false-positive inferior wall defects and their influence in defect reversibility patterns is currently being evaluated (*29*).

Previous studies have shown that teboroxime stress studies can be performed with a sensitivity and specificity comparable to ^{201}Tl when used in combination with exercise, whether by planar (*30–34*) or SPECT methods (*24,25,34*). In the study by Iskandrian et al. (*24*) using adenosine-induced hyperemia, there was 80% segmental agreement between teboroxime and thallium SPECT results. More recently, Serafini et al. (*35*) have reported a comparison of teboroxime and ^{201}Tl in 17 patients undergoing treadmill exercise, examined using a single-detector SPECT camera with modified step and shoot (or "pseudo-continuous") detector motion. Concordance between the two tracers was 94% for patients and 90% for segments, with both tracers detecting an equal number of normal and abnormal segments.

Study Limitations

Twenty-two patients in our study population had prior myocardial infarction. Thus, only 20 patients with coronary artery disease by angiography and no prior myocardial infarction were available for the assessment of diagnostic sensitivity. With respect to specificity, only seven patients had normal coronary angiograms. Consequently, the findings of a high sensitivity and moderate specificity must be considered preliminary.

Quantitation was not performed in this study, as normal limits for teboroxime studies have yet to be determined. It is possible that with quantitative analysis, different imaging times (e.g., 2–3 min versus 2–5 min) may result in significant differences in stress defect severity, a perfusion index which has been previously shown with ^{201}Tl to correlate with the degree of angiographic stenosis (*36–37*). We have previously shown (*18*) that teboroxime washout in ischemic regions is slowed compared to the normally perfused myocardium, which would explain the occasionally observed visually more severe stress defects in the 2–3-min images compared to the 2–5-min images (Fig. 7). Further studies will be required to determine which teboroxime imaging time yields defect severity which best correlates with the degree of angiographic lesion severity.

Since the rest injection was given 15 min following ade-

nosine stress, it is theoretically possible (although unlikely, due to the extremely short half-life of adenosine) that the myocardium remained in an "ischemic" state at the time of the rest teboroxime injection. The administration of nitroglycerine prior to resting injection may improve the assessment of the stress defect reversibility pattern, as has been previously shown with ^{201}Tl (*38*) and technetium sestamibi (*39*).

CONCLUSIONS

Our study established the recommended imaging parameters for a rapid back to back adenosine stress/rest teboroxime perfusion SPECT protocol. The results indicate that by combining adenosine-induced hyperemia with teboroxime and a triple-detector camera, stress followed by rest SPECT studies can be performed within 30 min. Interference from intense liver uptake remains problematic and necessitates rapid completion of imaging. In the majority of studies, however, images were readily interpretable, and the study protocol was observed to result in high sensitivity and normalcy rates for the detection of coronary artery disease. Back to back adenosine stress/rest teboroxime SPECT is technically demanding because of the limited imaging time available, and should be performed with precision and vigilant quality control.

ACKNOWLEDGMENTS

This work was supported in part by a grant from Squibb Pharmaceuticals and a grant from Medco Research, Inc., Los Angeles, CA. This work was presented in part at the 64th Annual Scientific Sessions, American Heart Association, Anaheim, CA, November 1991 and the 39th Annual Meeting of the Society of Nuclear Medicine, Los Angeles, CA, June 1992.

REFERENCES

1. Narra RK, Nunn AD, Kucynski BL, Feld T, Wedeking P, Eckelman WC. A neutral technetium-99m complex for myocardial imaging. *J Nucl Med* 1989;30:1830–1837.
2. Meerdink DJ, Leppo JA. Experimental properties of technetium-99m agents: myocardial transport of perfusion imaging agents. *Am J Cardiol* 1990;66:9E–15E.
3. Leppo JA, Meerdink DJ. Comparative myocardial extraction of two technetium-labeled BATO derivatives (SQ30217, SQ30214) and thallium. *J Nucl Med* 1990;31:67–74.
4. Leppo J, DePuey E, Johnson L. A review of cardiac imaging with sestamibi and teboroxime. *J Nucl Med* 1991;32:2012–2022.
5. Diamond GA, Forrester JS. Analysis of probability as an aid in the clinical diagnosis of coronary artery disease. *N Engl J Med* 1979;300:1350–1358.
6. Diamond GA, Forrester JS, Hirsch M, et al. Application of conditional probability analysis to the clinical diagnosis of coronary artery disease. *J Clin Invest* 1980;65:1210–1221.
7. Diamond GA. *CADENZA: computer-assisted diagnosis and evaluation of coronary artery disease.* Seattle: Software Cardiokinetics Inc.; 1985:1–35.
8. Ratib O, Huang HK. CALIPSO: an interactive software package for multimodality medical image analysis on a personal computer. *J Med Im* 1989; 3:205–216.
9. Kiat H, Berman DS, Maddahi J, et al. Late reversibility of tomographic myocardial thallium-201 defects: an accurate marker of myocardial reversibility. *J Am Coll Cardiol* 1988;12:1456–1463.
10. Yang LD, Berman DS, Kiat H, et al. The frequency of late reversibility in SPECT thallium-201 stress-redistribution studies. *J Am Coll Cardiol* 1990; 15:334–340.
11. True Epistat Statistical Software. Epistat services. Richardson, TX.
12. Takemoto K, Berman DS, Kiat H, et al. Back to back adenosine/rest Tc-99m teboroxime scintigraphy: a feasibility study [Abstract]. *Circulation* 1991;84:II;315.
13. O'Connor MK, Kelly BJ. Evaluation of techniques for the elimination of "hot" bladder artifacts in SPECT of the pelvis. *J Nucl Med* 1990;31:1872–1875.
14. Friedman J, Van Train K, Maddahi J, et al. "Upward creep" of the heart: a frequent source of false positive reversible defects on Tl-201 stress-redistribution SPECT [Abstract]. *J Nucl Med* 1986;27:899.
15. Wilson RF, Wyche K, Christensen BV, Zimmer S, Laxson DD. Effect of adenosine on human coronary arterial circulation. *Circulation* 1990;82: 1595–1606.
16. Burns RJ, Wright L. Three-minute acquisition of exercise ^{99m}Tc teboroxime cardiac SPECT with a single-head detector [Abstract]. *J Nucl Med* 1991; 32:929.
17. Stewart RE, Heyl B, O'Rourke RA, Blumhardt R, Miller DD. Demonstration of differential post-stenotic myocardial technetium-99m teboroxime clearance kinetics after experimental ischemia and hyperemic stress. *J Nucl Med* 1991;32:2000–2008.
18. Chua T, Kiat H, Germano G, Palmas W, Takemoto K, Friedman J, Berman DS. Tc-99m teboroxime regional myocardial washout in subjects with and without coronary artery disease. *Am J Cardiol* 1993: in press.
19. Bok BD, Bice AN, Clausen M, Wong DF, Wagner Jr HN. Artifacts in camera based single photon emission tomography due to time activity variation. *Eur J Nucl Med* 1987;13:439–442.
20. Links JM, Frank TL, Becker LC. Effect of differential tracer washout during SPECT acquisition. *J Nucl Med* 1991;32:2253–2257.
21. O'Connor MK, Cho DS. Rapid radiotracer washout from the heart: effect on image quality in SPECT performed with a single-headed gamma camera. *J Nucl Med* 1992;33:1146–1151.
22. Nakajima K, Shuke N, Taki J, et al. A simulation of dynamic SPECT using a radiopharmaceutical with rapid clearance. *J Nucl Med* 1992;33:1200–1206.
23. Rumsey WL, Rosenspire KC, Nunn AD. Myocardial extraction of teboroxime: effects of teboroxime interaction with blood. *J Nucl Med* 1992;33:94–101.
24. Fleming RM, Kirkeeide RL, Teagtmeyer H, Adyanthaya A, Cassidy DB, Goldstein RA. Comparison of technetium-99m tomography with automated quantitative coronary arteriography and thallium-201 tomographic imaging. *J Am Coll Cardiol* 1991;17:1297–1302.
25. Iskandrian AS, Heo J, Nguyen T, et al. Tomographic myocardial perfusion imaging with technetium-99m teboroxime during adenosine-induced coronary hyperemia: correlation with thallium-201 imaging. *J Am Coll Cardiol* 1992;19:307–312.
26. Rozanski A, Diamond GA, Berman D, Forrester JS, Morris D, Swan HJC. The declining specificity of exercise radionuclide ventriculography. *N Engl J Med* 1983;309:518–522.
27. Rozanski A, Diamond GA, Forrester JS, Berman DS, Morris D, Swan HJC. Alternative referent standards for cardiac normality. Implications for diagnostic testing. *Ann Intern Med* 1984;101:164–171.
28. Kiat H, Berman D, Wong F, et al. The normalcy rate of quantitative stress Tl-201 myocardial perfusion SPECT [Abstract]. *J Nucl Med* 1991;32:959.
29. Germano G, Chua T, Areeda JS, Kiat H, Berman DS. Hepatic uptake creates artifactual defects in 99mtc myocardial spect images: a quantitative phantom analysis [Abstract]. *J Nucl Med* 1993;34:189P.
30. Johnson LL, Seldin DW. Clinical experience with technetium-99m teboroxime, a neutral, lipophilic myocardial perfusion agent. *Am J Cardiol* 1990; 66:63E–67E.
31. Seldin DW, Johnson LL, Blood DK, et al. Myocardial perfusion imaging with technetium-99m SQ30217: comparison with thallium-201 and coronary anatomy. *J Nucl Med* 1989;30:312–319.
32. Hendel RC, Mcsherry B, Karimeddi M, Leppo JA. Diagnostic value of a new myocardial perfusion agent, teboroxime (SQ30217), utilizing a rapid planar protocol: preliminary results. *J Am Coll Cardiol* 1990;16:855–861.
33. Taillefer R, Freeman M, Greenberg D, et al. Detection of coronary artery disease: comparison between ^{99m}Tc-teboroxime and 201-thallium planar myocardial perfusion imaging (Canadian Multicenter Clinical Trial) [Abstract]. *J Nucl Med* 1991;32:919.
34. Iskandrian AS, Heo J, Nguyen T, Mercuro J. Myocardial imaging with Tc-99m teboroxime: technique and initial results. *Am Heart J* 1991;121:889–894.
35. Serafini A, Topchik S, Jimenez H, Friden A, Ganz WI, Sfakianakis GN. Clinical comparison of technetium-99m teboroxime and thallium-201 utilizing a continuous SPECT imaging protocol. *J Nucl Med* 1992;33:1304–1311.
36. Matzer L, Kiat H, Van Train K, et al. Quantitative severity of stress thallium-201 myocardial perfusion single-photon emission computed tomography defects in one-vessel coronary artery disease. *Am J Cardiol* 1993;72: 273–279.

37. Hadjimiltiades S, Watson R, Hakki A, Heo J, Iskandrian AS. Relation between myocardial thallium-201 kinetics during exercise and quantitative coronary angiography in patients with one vessel coronary artery disease. *J Am Coll Cardiol* 1989;13:1301–1306.
38. Medrano R, Mahmarian JJ, Verani M. Nitroglycerin before reinjection of thallium-201 enhances detection of reversible hypoperfusion via colleteral blood flow: a randomized, double blind, parallel, placebo-controlled trial [Abstract]. *J Am Coll Cardiol* 1993;21:221A.
39. Galli M, Marcassa C, Silva P, Zoccarato O, Campini R, del Lavoro C. Improvement of resting ^{99m}Tc-sestamibi myocardial uptake by acute nitroglycerin administration [Abstract]. *J Am Coll Cardiol* 1993;21:221A.

(continued from page 5A)

FIRST IMPRESSIONS

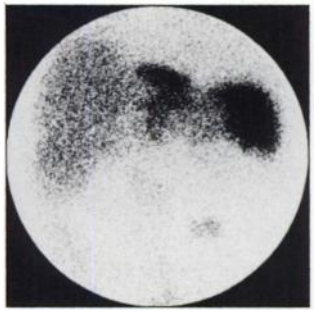

FIGURE 1. Initial ^{111}In-WBC image of the upper abdomen performed 1 mo after initial surgery demonstrates a wound abscess, a colostomy site and no evidence of splenic activity.

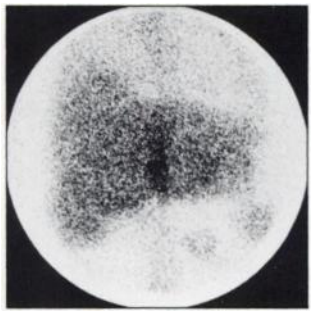

FIGURE 2. Anterior ^{111}In-WBC image of the upper abdomen from the second study shows a wound abscess, a splenic-bed abscess and the colostomy site.

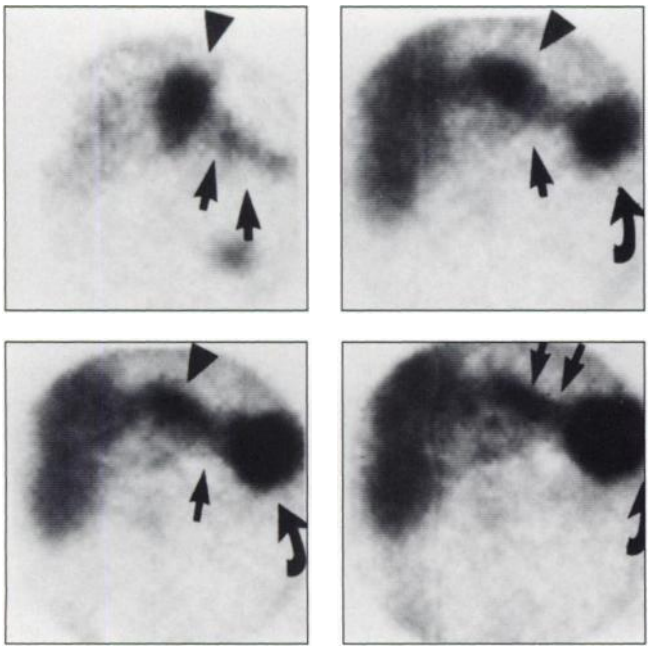

FIGURE 3. Coronal ^{111}In-WBC SPECT images of the upper abdomen from the second study demonstrates a wound abscess (arrow heads), a communicating tract (straight black arrows) and a splenic-bed abscess (curved arrows).

PURPOSE

The patient is a 66-yr-old man who had repair of an aortic aneurysm about 2 mo prior to the current examination. The postoperative period was complicated by retroperitoneal bleeding, hypotension, persistent fever and ischemic bowel, for which a left hemicolectomy was performed. Ten days later, the patient underwent a splenectomy for splenic infarcts. The fever continued to persist, and the patient underwent a white blood cell (WBC) scan 1 mo after the initial surgery. The scan (Fig. 1) showed increased WBC activity in the abdominal wound consistent with a wound abscess. A colostomy stoma also was seen.

Normal splenic WBC activity was not seen because of splenectomy. The second scan (Fig. 2), performed during the current examination, shows a large spleen-shaped collection of intense WBC activity in the splenic bed, which on first impression could easily pass for normal splenic activity. The history of a splenectomy and correlation with the earlier WBC scan makes the diagnosis of an abscess in the splenic bed quite apparent. The abscess was drained on the same day under CT guidance, and 180 cc of pus was removed. A moderately intense collection of WBC activity in the upper end of the midline abdominal wound is seen again with a persistent wound abscess. The colostomy stoma is also seen. A SPECT scan of the abdomen revealed a communication between the wound abscess and splenic bed abscess just beneath the diaphragm (Fig. 3).

Without the history of a splenectomy, how many of you made the diagnosis of a splenic-bed abscess in addition to wound abscess? We did not! The purpose of this study is to illustrate the critical importance of appropriate history and correlation with prior, or other, imaging studies in making the proper diagnosis in complex clinical circumstances.

TRACER

^{111}In-WBC.

ROUTE OF ADMINISTRATION

Intravenously.

TIME AFTER INJECTION

24 hours.

INSTRUMENTATION

ROTA dual head (Siemens).

CONTRIBUTORS

Shoba Desai, David Yuillle and Don Spiegelhoff.

INSTITUTION

St. Luke's Medical Center, Milwaukee, Wisconsin.